Journal of Medical Systems (2019) 43: 307
https://doi.org/10.1007/s10916-019-1423-1

IMAGE & SIGNAL PROCESSING

Efficient Image De-Noising Technique Based on Modified Cuckoo Search Algorithm

Sakthidasan @ Sankaran K[1] · Vasudevan N[1] · Kumara Guru Diderot P.[1] · Nagarajan V[2]

Received: 28 March 2019 / Accepted: 11 July 2019 / Published online: 16 August 2019

Abstract

The image restoration has emerged as a very vital investigation technique in the domain of the image processing. The underlying motive behind the image restoration is devoted to the augmentation of the perceived visual impact of image so as to make it almost identical to the original image. A host of exploration approaches are now in vogues which are intended to steer clear of the noise, thereby regaining the images with original quality. In our earlier research, two distinct noise elimination methods like the (OGHP) and SURE shrinkage were effectively employed for the purpose of denoising, though the relative PSNR and SSIM efficiencies did not come up to the desired level. In the innovative approach envisaged in the document, at the outset, the noise is included by means of two processes like the salt and pepper and impulse noise. Subsequently, the pre-processing methods are performed with the able assistance of two novel filters such as the adaptive median filter and adaptive fuzzy switching. Thereafter, the preprocessed image is furnished to the succeeding function of noise elimination like the (OGHP) and SURE shrinkage. In the course of the OGHP noise elimination technique, the GHP constraints are optimized by employing the Cuckoo Search Algorithm. Thereafter, the noise-eliminated image is effectively estimated with the help of the Discrete Wavelet Transform (DWT). The consequential noiseless images are subjected to the image restoration procedure by efficiently employing the AGA approach. The cheering performance outcomes chant the success stories of the novel image restoration method, highlighting its superlative efficiency. Moreover, the efficacy of the innovative approach is assessed by means of a set of noise-polluted images and contrasted with the modern noiseless image restoration technique.

Keywords Image de-noising · Image restoration · Adaptive median filter · Adaptive genetic algorithm (AGA) · MODIFIED cuckoo search algorithm (MCSA) · Discrete wavelet transform (DWT) · Adaptive genetic algorithm (AGA)

Introduction

The images are generally designed for the purpose of exhibiting fruitful data. It is often found that the original images are habitually spoilt on account of certain disarray at the time of image acquirement. Hence, the vital motive of the image restoration is concerned with the function of either "compensating for" or "undoing" the inherent deficiencies which ultimately results in the degradation of the image concerned [1]. The degradation generally appears in many versions like the motion blur, noise, and camera mis-focus. In the case of the motion blur, it is easy to arrive at an excellent evaluation of the actual blurring function and carry out the process of "undoing" the blur to effectively regain the original image. However, where the image is tainted by noise, the only possible option to perform the process which duly compensates for the degradation already happened. In the current investigation, it is planned to launch novel methods and

This article is part of the Topical Collection on *Image & Signal Processing*

✉ Sakthidasan @ Sankaran K
sakthidasan.sankaran@gmail.com

Vasudevan N
drvasudevan93@gmail.com

Kumara Guru Diderot P.
diderotpec2007@gmail.com

Nagarajan V
nagarajanece31@gmail.com

[1] Department of Electronics and Communication Engineering, Hindustan Institute of Technology and Science, Chennai 603103, India

[2] Department of Electronics and Communication Engineering, Adhiparasakthi Engineering College, Melmaruvathur 603319, India

execute various approaches extensively used in the domain of the image processing with the intention of effectively regaining the images [2].

In the ever-zooming realm of the image processing, the image restoration enacts a very vital role for the purpose of attaining excellent quality image from the noise-polluted or tainted image. In this regard, the denoising appears on the arena as the most appealing image restoration approach applied to get rid of the noise persisting in the input image [3]. The superfluous noise in the images has to be drastically reduced so as to improve the efficiency of the image restoration performance well-ahead of the restoration procedure in the image pre-processing technique. In fact, the image denoising contributes its mite by performing very vital functions in various facets [4].

It is with the ultimate objective of eliminating the noise from a degraded image in the course of attainment and communication that the image de-noising is habitually utilized. While taking due care in preserving the vital signal features intact, the image de-noising is elegantly executed to eliminate the additive noise [5]. The most critical feature for any noise-polluted data is concerned with the deployment of an ideal denoising technique for the purpose of compensation. An added issue cropping up in the process of the de-noising is to appropriately address the 'staircase effect' simultaneously conserving the sharpness and convexity of the image [6].

In this connection, the Wavelet transform (WT) projects itself as an ideal candidate dedicated for the purpose of the disintegration and rebuilding of the multi-dimensional signals for their investigation, resolution enrichment and additional processing [7]. The noise elimination by means of diverse versions of the low pass filtering approaches has established itself as a very significant topic of exploration in the realms of the digital image and signal processing. Incidentally, the term 'image restoration' refers to the process of denoising a tainted image. The fundamental objective of the restoration technique is concerned with the regaining of the original image from the perceived tainted image. Nowadays, the image restoration techniques are extensively employed to design the degradation procedure and perform a roughly inverse procedure to the tainted image for the purpose of regaining the original image [8].

The efficacy of the corresponding restoration methods is squarely dependent on the accessibility and totality of the knowledge regarding the impulse deprivation procedure and on the configuration of the filtering technique. The linear filter is sufficient enough to get rid of the noise in respect of a bandwidth constrained additive noise such as the Gaussian noise from the tainted images. For the purpose of effectively eradicating the related deficiencies, the non-linear filters such as the median filter are habitually utilized to denoise the Salt & Pepper noise from the tainted image. The median filter, in essence, represents a computationally effectual nonlinear filter intended for the denoising of the impulse noise in addition to conserving the edges. A feast of diverse image restoration approaches have been fascinatingly flagged off in the literary arena which is intended for the purpose of the digital image processing [9].

Related works

Lei Yang *et al.* [10] elegantly envisaged an innovative feature-preserving non-local means approach for denoising the tainted images so as to perk up the feature revival and particle recognition. The most widely employed non-local means filter was found to be unsuitable for the noise-polluted bio-logical images encompassing trivial facets of significance as the image noise invariably thwarted the appropriate estimation of the accurate coefficients for the purpose of averaging, resulting in the over-smoothing and parallel artifacts. They successfully tackled the issue by generating a particle feature probability image, and illustrated the fact the novel filter was competent to realize superior levels of the peak signal-to-noise ratio in the denoised images and was well-equipped with the requisite skills in effectually detecting the weak particles when applied to artificial data. Further, they unequivocally established the fact that their feature-preserving non-local means filter was able to considerably cutback the threshold of imaging conditions essential for the achievement of significant data.

Tzu-Chao Lin *et al* [11] charismatically launched a novel decision-based fuzzy averaging (DFA) filter noise detector. The novel filter was competent to efficiently address the impulsive noise, and a mixture of Gaussian and impulsive noise. The combination confidence value represented the decision rule in respect of the D–S noise detector. Further a fuzzy averaging technique was also brilliantly brought in, where the weights were built by means of a pre-determined fuzzy set, for the purpose of attaining the noise abolition. Further, a straightforward second-pass filter was effectively utilized to augment the efficiency of the ultimate final filtering accomplishment. The enthusing test upshots effectively exhibited the exemplary efficacy of the novel DFA filter in the compression of the suppressing impulsive noise and also the mixture of the Gaussian and impulsive noise, together with a significant enhancement in the apparent image excellence.

Chul Lee *et al.* [12] were instrumental in efficiently launching an innovative nonlocal minimum mean square error (MMSE) image denoising technique. In their novel approach, they investigated the nonlocal neighbors from an external database and also the complete input image to boost the efficiency in execution even in cases where a noise-polluted block is not likely to contain identical blocks within the image. In view of the fact that the extensive search range necessitated a greater computational load, they deftly devised a probabilistic tree-based search technique to considerably cutback the

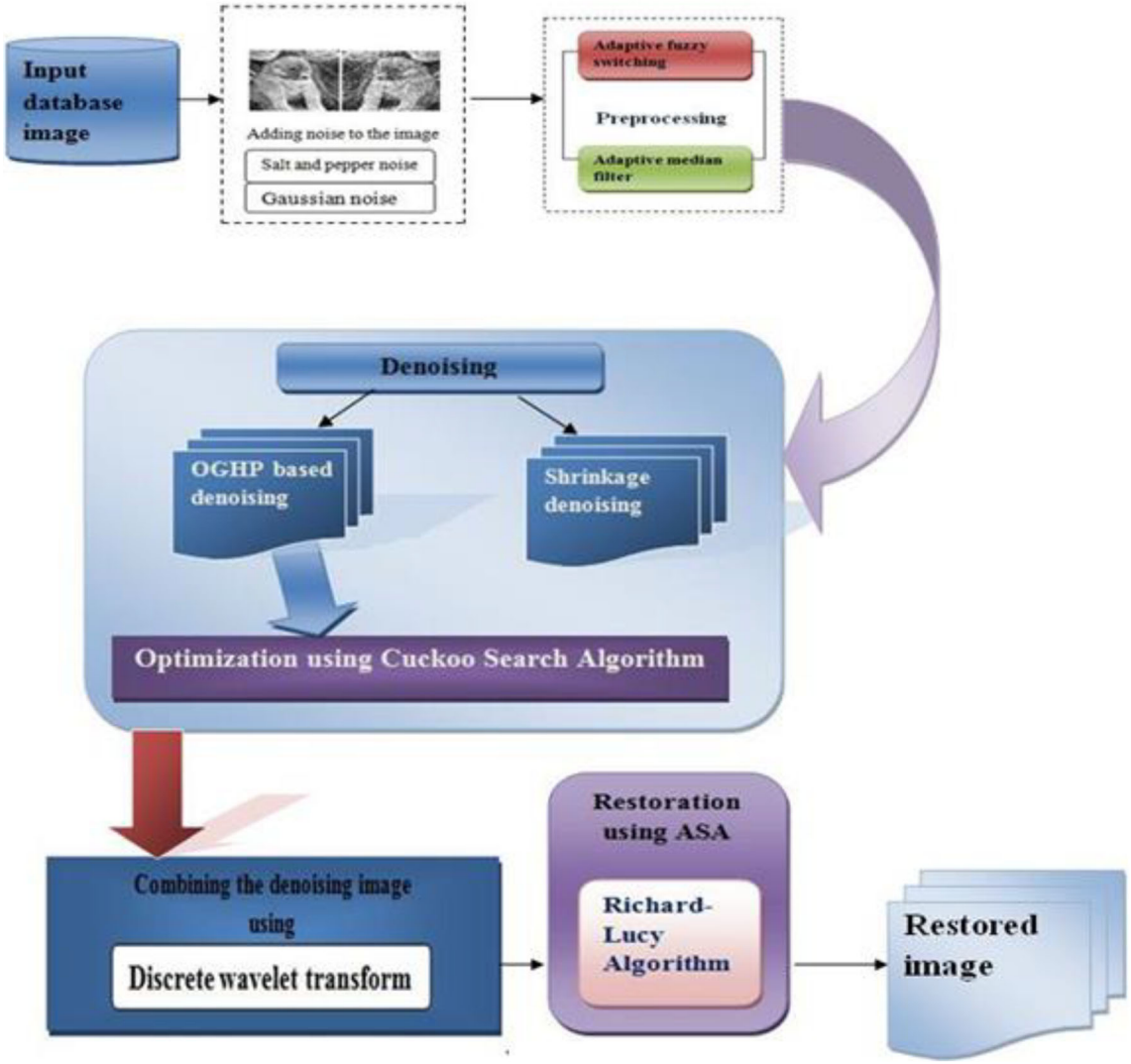

Fig. 1 Architecture of the Proposed Image Restoration Technique

computational complication. The remarkable replication results have revealed the fact that the novel technique was well-geared to exhibit further exemplary denoising performance in relation to that of the traditional nonlocal means filter.

An innovative and powerful pattern for the purpose of the image and video de-noising, de-blurring, and super resolution reconstruction was effectively green-signaled by Haichao Zhang *et al.* [13]. The overall test outcomes on the mutual single images and pragmatic video progressions illustrated with perfect precision that the novel structure gained a convincing edge over the earlier investigations both in qualitative and quantitative aspects.

A Fenchel duality root from dictionary learning (FD-DL) technique for the restitution of the noise-tainted images was brilliantly brought to limelight by Shanshan Wang *et al.* [14]. By way of the inhibited concern for the additive white Gaussian noise, the sparse image illustration was planed as an l_2-l_1 reducing challenge, deftly deploying an oversimplification of Fenchel's duality thesis and effectively resolved depending on the improved Lagrangian frame-work whose dual configuration was established. Further, the fantastic technique was assessed and compared with four diverse sophisticated approaches such as the integration of the local pixel grouping-principal element examines, K-singular value disintegration, the method of optimal directions, on grayscale natural images and the beta process factor examine. It was crystal from the outstanding outputs released by various algorithms that the FD-DL technique was able to reach the top of the list by effectively enriching the excellence of the image and also because of its inherent skills in regard to the restoration of the tainted image which when during the comparison with the other four popular techniques, scaled a significant edge over them.

Fig. 2 Sample input images

Wishing Dong *et al.* [15] deeply discussed the issue of the sparse coding noise and efficiently elucidated how the ultimate motive of the image restoration was able to put a hold on the sparse coding noise. Further they effectively discouraged nonlocal self-similarity of the image to successfully achieve the superior appraisal of the sparse coding coefficients of the genuine image for integrating the sparse coding coefficients of the experimental image to the related evaluation, for achieving the purpose. While their extensive experiments on diverse classes of image restoration challenges such as the denoising, de-blurring and super-resolution, authenticated the generalization and hi-tech performance of the projected NCSR technique, the self-styled non-locally centralized sparse representation (NCSR) pattern emerged as simple as the typical sparse representation model.

The Wavelet-based sparse reduced-rank regression (WSRRR) technique for the hyper-spectral image restoration was brilliantly brought to limelight by Behnood Rasti*et al.* [16]. The innovative approach was dependent on alleviation of a sparse stipulation hassle linked to an orthogonality constraint. With the intention of scaling down the dilemma a cyclic descent-type technique was elegantly employed. Taking inspiration from Stein's unprejudiced risk inference, they pressed the green light for a new approach for selecting the tuning constraints. The suggested technique was efficiently evaluated by means of the signal-to-noise ratio and spectral angle distance for a simulated corrupted data set which were classified as efficiencies for a bona fide data set. By means of employing a minimal number of sparse components it was established that the hyper-spectral image could be regained. In their projected hypothesis, two distinct classifiers such as the support vector machines and random forest were significantly employed. Their anticipated method was compared and contrasted with the parallel restoration approaches which upheld the superiority and significance of the WSRRR for the replicated tainted data set.

Proposed image restoration technique

The innovative technique flows through the following five phases.

1. The preprocessing
2. The denoising employing the OGHP

- The optimization employing the optimized Cuckoo Search technique

3. The denoising employing the shrinkage
4. The evaluation employing the DWT.
5. The image restoration employing the AGA

Preprocessing

The noise represents the adverse impact generated in the image which ultimately leads to the diminution in the quality of the image. Hence, it is all the more essential to get rid of the noise from the image. In the novel approach, for the purpose of steering clear of the noise, two distinct and effective filters are employed which are shown below.

- The Adaptive Median Filter
- The Adaptive Fuzzy Switching

Prior to the preprocessing of the input image, two diverse categories of noise are added to the image and they are known as the salt & pepper and the Gaussian noise.

Adaptive median filter

The Adaptive Median Filtering characterizes a nonlinear low pass filter which is sufficient for the purpose of eliminating the

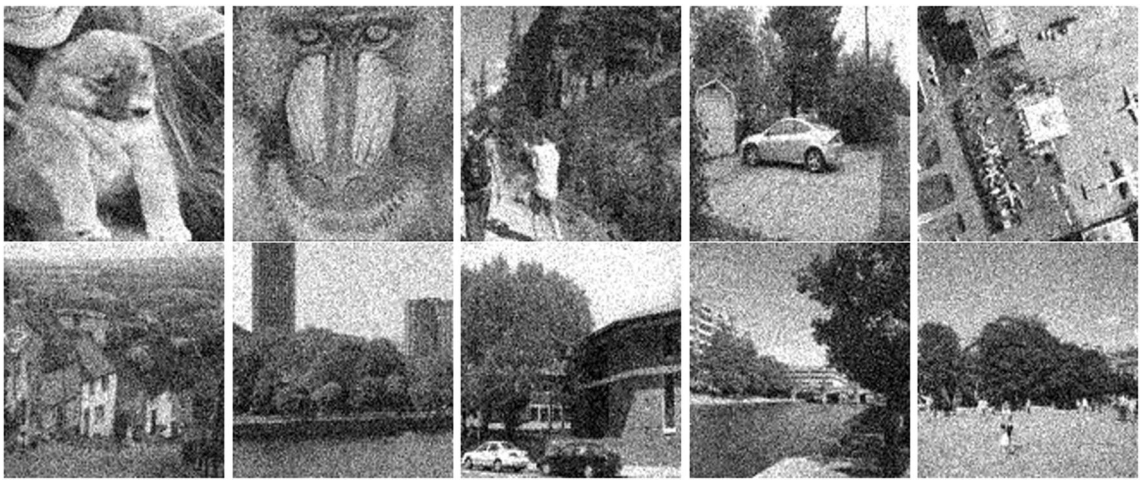

Fig. 3 Gaussian noise added images

outliers which constitute the intense pixel values in an image. The input image $R_d = \{f_{i^1}, f_{i^2}, f_{i^3} \cdots f_{i^j}\}; j = 1, 2, 3, \cdots N$ is fed to the Median filter.

The adaptive median filter is performed on the images $r_d(f, s)$ which are tainted by the (Gaussian noise) and subsequently a noiseless image is achieved as an output. The gradual procedure of the adaptive median filtering in the noise elimination is effectively pictured as follows.

Step 1: Initialize the window w size w_z.
Step 2: Examine whether the center pixel $p_{cen}(r, s)$ within w is noise-contaminated. If the pixel $p_{cen}(f, s)$ is noise-polluted proceed to step 3. Else, slide the window to the successive pixel and replicate step 1.
Step 3: Organize the whole pixels within the window $w$in an increasing order and locate the minimum ($p_{\min}(f, s)$), median ($p_{med}(f, s)$), and maximum ($p_{\max}(f, s)$) values.
Step 4: Evaluate whether $p_{med}(r, s)$ is noise-polluted. (i.e.) $p_{\min}(f, s) < p_{med}(f, s) < p_{\max}(f, s)$.

If the median value range falls in between the minimum and maximum means the pixel is free from noise and then proceed to step 5. Else, $p_{med}(f, s)$ is a noise-polluted pixel and hence proceed to step 6.

Step 5: Substitute the related centre pixel in output image with $p_{med}(f, s)$ and proceed to step 8.
Step 6: Examine whether all the other pixels are noise-polluted. If yes then enlarge the window size by 2 and return to step 3. Else, proceed to step 7.
Step 7: Substitute the center pixel of the image with the noiseless pixel which is the nearest one of the median pixel $p_{med}(f, s)$.
Step 8: Reorganize window size w_z and center of window to the succeeding pixel.

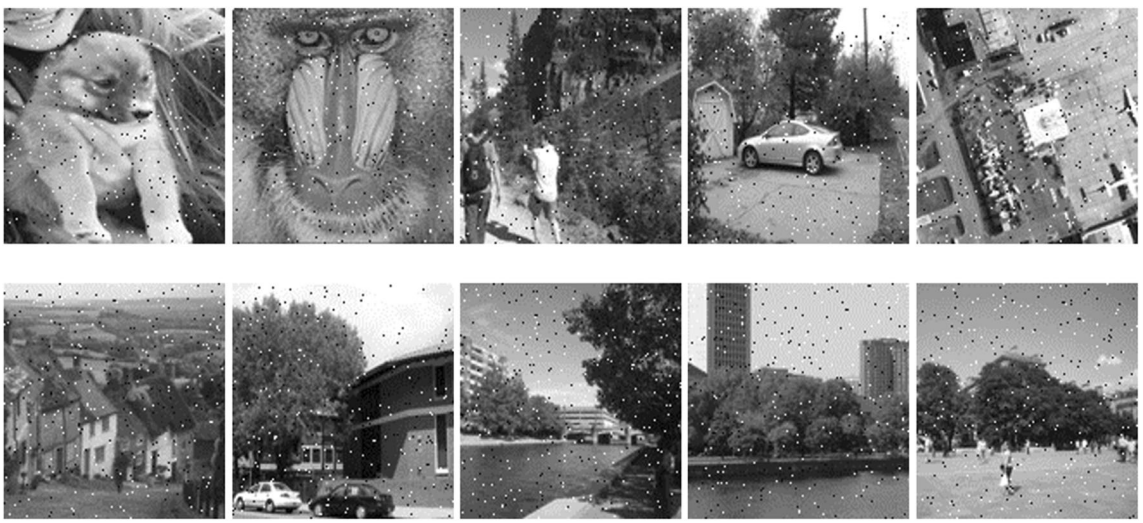

Fig. 4 Salt and pepper noise added images

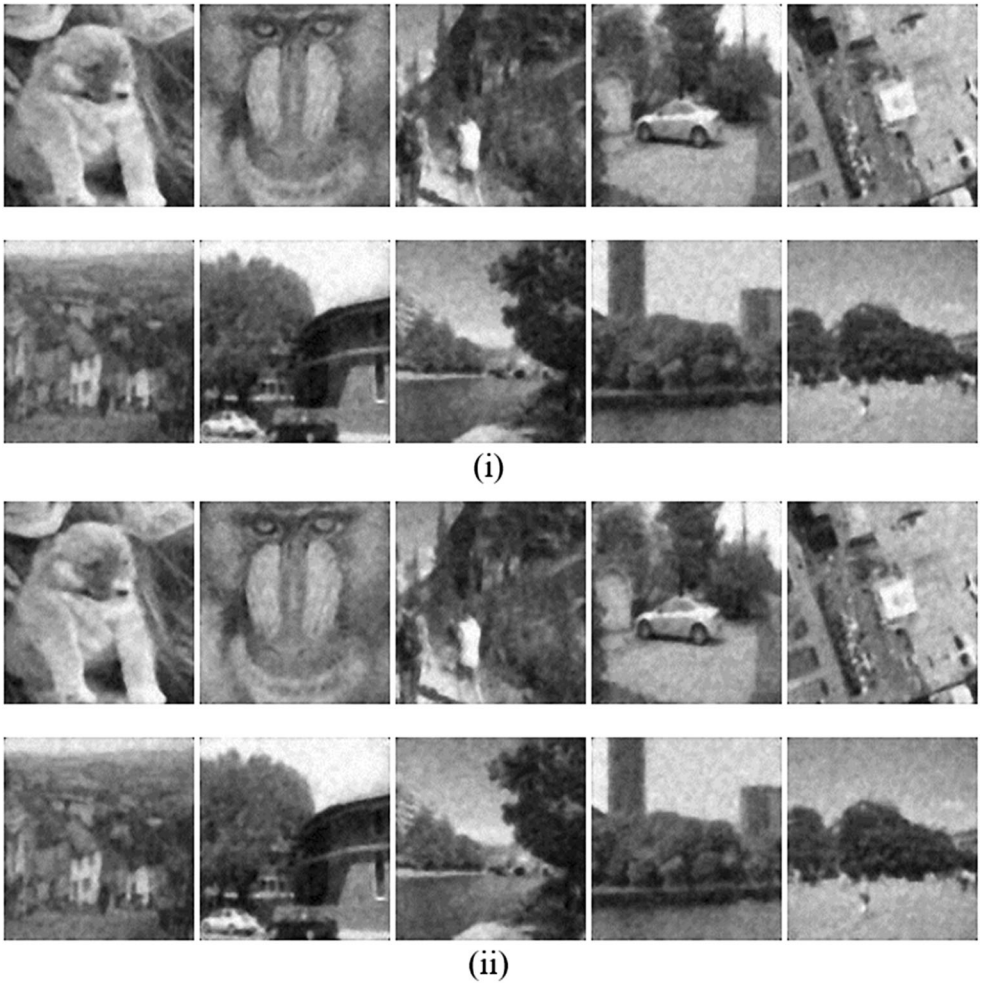

Fig. 5 De-noised Images (i) Gaussian Noise Removed Image (ii) Impulse Noise Removed Image

Step 9: Replicate the above steps till all the pixels are processed.

Fuzzy switching method

Of late, in the literature regarding the denoising, the fuzzy switching median filter has emerged as one of the most widely used techniques. Habitually, it contains two specific phases. The initial phase is the noise recognition phase which is essential before proceeding to the fuzzy switching technique. In accordance with the noise identification, it is possible to differentiate between the "suspicious noise pixels" and the "noise free pixels". Then, the fuzzy switching technique is performed for the cancellation module as detailed below.

$$d(i+k+1) = \left[X(i+k, j+1) - X(i,j)\right. \tag{1}$$

Then the constraint $D(i,j)$ characterizing the local data is defined as the maximum absolute luminance difference in the filtering window as shown in Eq. 4 given below.

$$D(i,j) = \max\{d(i+k, j+1)\} \tag{2}$$

In accordance with $D(i,j)$ pixels in the image X is segmented into three diverse categories such as the "noise free pixels", "suspicious noise free pixels" and the "suspicious noise pixels". The fuzzy reasoning used is illustrated in Fig. 1 and the function $f(i,j)$ is illustrated by means of Eq. 5 shown as follows.

$$\begin{aligned} f(i,j) &= \left\{0, D(i,j), T_1\right. \\ f(i,j) &= \left\{\frac{D(i,j) - T_1}{T_2 - T_1}; T_1 \le D(i,j) \le T_1\right. \\ f(i,j) &= \left\{1, D(i,j) \ge T_2\right. \end{aligned} \tag{3}$$

The consequential noiseless image is thereafter furnished to the image denoising procedure.

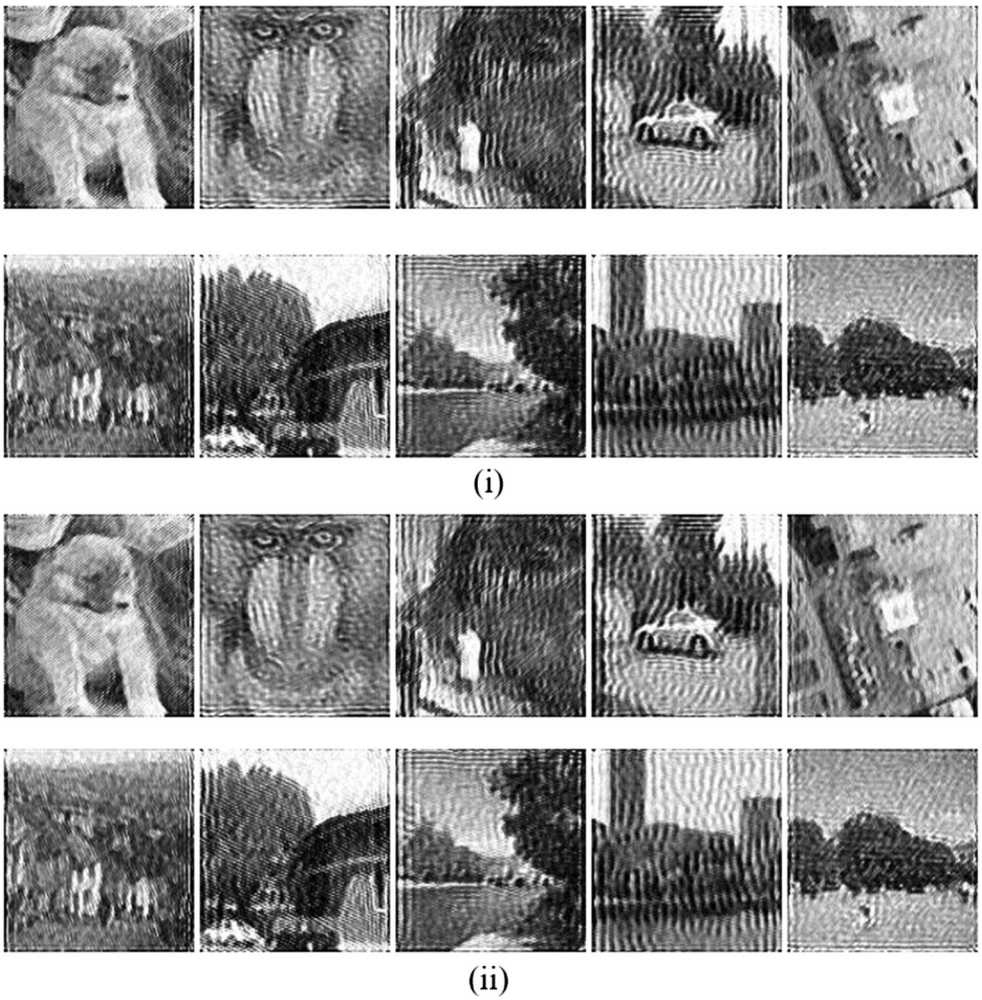

Fig. 6 Restored Images (i) Gaussian Noise Removed Image (ii) Impulse Noise Removed Image

Denoising optimized gradient histogram preservation (GHP)

Here, the image denoising is modeled by the gradient histogram preservation together with the sparse non-local regularization, and an effective histogram specification technique to resolve the anticipated model for the purpose of the texture enhanced image denoising.

In respect of a specified noiseless image $n(x)$, the noisy observation $n(y)$ of $n(x)$ is habitually represented by means of the following Eq. 6.

$$n(y) = n(x) + g(n) \tag{4}$$

Here $g(n)$ represents the noise with zero mean and standard deviation σ. The vital motive of the image denoising is to assess the desired image $n(x)$ from $n(y)$.With the result, there emerges a well-ordered iterative histogram specification technique to resolve the model in Eq. (2). Further, from the shrinkage dependent noise riddance process, the denoised image I_2 is effectively attained. As a result the optimized Gradient Histogram Preservation (OGHP) dependent denoised images I_1 and shrinkage dependent denoised image I_2 are incorporated by the Discrete wavelet transform. Obtaining the denoised image using GHP process is detailed in the previous paper except the optimization process.

Gradient histogram preservation optimized using MCSA

Principle behind modified cuckoo search algorithm

Each cuckoo bird lays a solitary egg at a time when it is abandoned into an arbitrarily selected nest. The optimum nest with the excellent quality eggs is carried over to the successive generations. The number of host nests is observed to be stagnant and a host is capable of locating an alien egg with a probability (Pa) [0, 1], whose existence ultimately leads to either discarding the egg or nest by

Table 1 Proposed and different filtering methods PSNR value of three Different Noise Variance levels 0.02, 0.05 and 0.07 (i) Gaussian Noisy images (ii) Impulse Noisy images

(i)

Noise Variance (σ^2)	PSNR					
	Noise Image (in dB)	Existing technique	Existing Shrinkage	Existing GHP	Hybrid Filter with AGA	Proposed
0.02	71.51	81.5444	77.8646	79.6598	75.757	82.87372
	71.51	81.3399	77.8208	79.6522	75.5396	82.58442
	71.29	80.4283	77.4515	78.8225	74.6493	82.3769
	71.02	82.2639	78.0416	80.2421	76.4599	81.37502
	71.28	81.9159	77.9964	79.9748	76.1183	83.17184
0.05	67.917645	79.5444	75.9646	77.6598	73.757	80.02162
	67.910586	79.3399	75.8208	77.6522	73.5396	79.65066
	67.894259	78.4283	75.9515	76.8225	72.6493	79.72528
	67.3930	80.2639	76.0916	78.2421	74.4599	78.92053
	67.6509393	79.9159	75.9864	77.9748	74.1183	80.22203
0.07	67.9176451	79.0444	75.2646	77.0598	73.557	78.81039
	67.9105863	78.6599	75.6208	77.1522	73.0315	79.81039
	67.8942591	78.4283	75.2515	76.9225	72.0124	80.81039
	67.3930042	80.02639	75.9916	77.2421	74.21549	81.81039
	67.6509393	79.5159	75.1264	76.9748	73.1183	82.81039

(ii)

Noise Variance (σ^2)	PSNR					
	Noise Image (in dB)	Existing Result	Existing Shrinkage	Existing GHP	Hybrid Filter with AGA	Proposed
0.02	76.07492241	82.5444	79.6598	81.5444	77.0737	89.08816
	76.5085284	82.3399	79.6522	81.3399	77.508	91.14094
	75.96744523	82.4283	78.8225	80.4283	76.96	87.51328
	76.58491914	83.2639	80.2421	82.2639	77.58491	84.21841
	76.36264045	82.9159	79.9748	81.9159	77.2025	91.85337
0.05	72.23199534	80.5444	77.6598	79.5444	75.9646	88.57738
	72.3797997	80.3399	77.6522	79.3399	75.8208	90.64813
	71.88227318	79.4283	76.8225	78.4283	75.9515	87.41496
	72.44685678	80.2639	78.2421	80.2639	76.0916	83.71736
	72.81821541	81.9159	77.9748	79.9159	75.9864	91.39508
0.07	70.8745187	81.0444	77.0598	79.0444	75.0737	88.27244
	70.39593524	80.6599	77.1522	78.6599	75.508	90.36898
	70.72301563	80.4283	76.9225	78.4283	75.96	86.91137
	70.72126683	81.02639	77.2421	80.02639	75.58491	83.58675
	71.05543201	80.5159	76.9748	79.5159	75.2025	91.01249

the host bird. It is pertinent to note that each egg in a nest characterizes a solution while a cuckoo egg symbolizes a novel solution in which the ultimate motive is to substitute the feeble fitness solution by a novel one.

The flowchart for the CSA is effectively exhibited below together with the vital steps:

Step 1: Bring in a random population of n host nests, I_d

Step 2: Achieve a cuckoo arbitrarily by Levy flight conduct, d

Step 3: Evaluate its fitness function, F_d

Step 4: Choose a nest arbitrarily among the host nests termed as j and evaluate its fitness, F_j

Step 5: If $F_d < F_j$ then substitute j by the new solution otherwise let j be the solution.

Step 6: Abandon a tiny proportion of Ax of the worst nest by constructing new ones at the new locations by employing the Levy flights.

Step 7: Maintain the current optimum nest, Return to Step (2) if T (Current Iteration) < MI (Maximum Iteration).

Step 8: Locate the optimum solution.

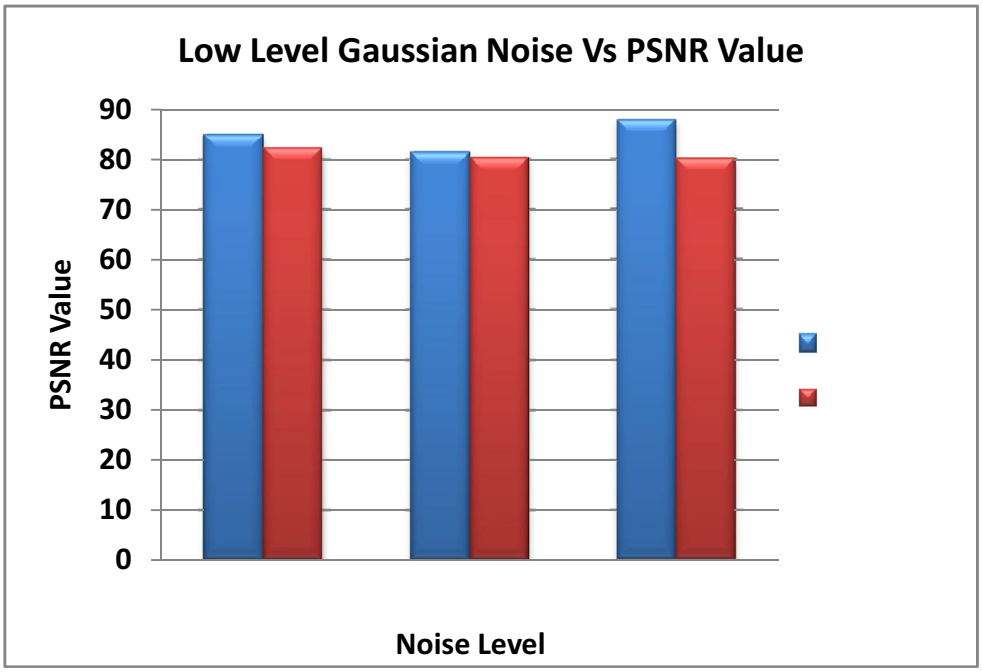

(i)

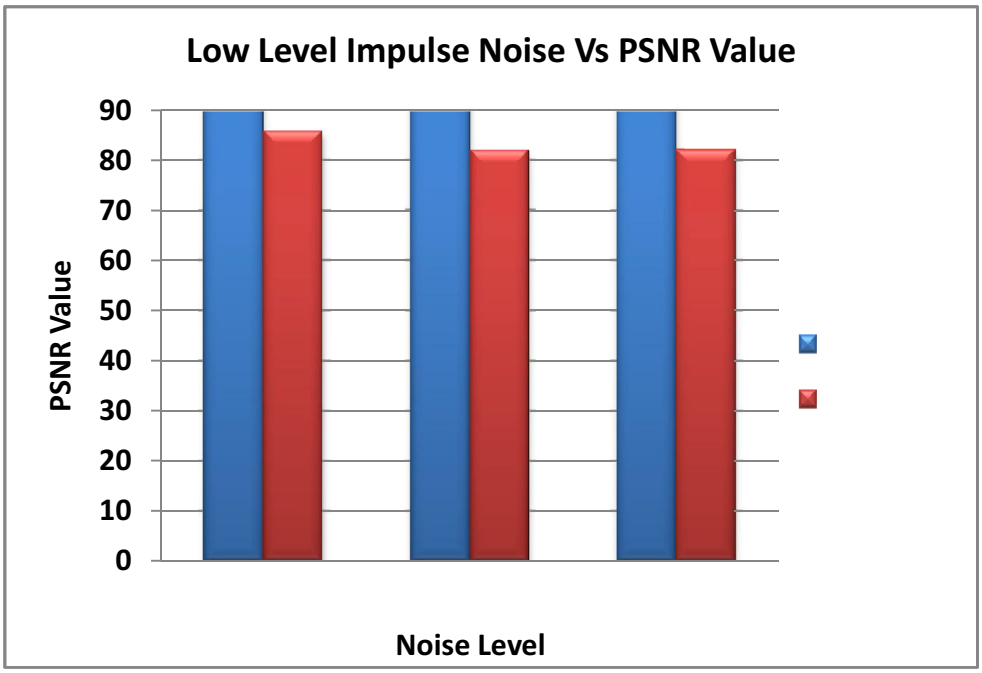

(ii)

Fig. 7 Comparison of noise removal performance of the proposed technique with that of the existing techniques (i) Gaussian Noise (ii) Impulse Noise

In this regard, the most vital phases involved in the CSA include the Initialization, where an arbitrary population of n host nest ($I_d = 1, 2, 3...n$). ii) is brought in, and the Levy Flight Behaviour in a cuckoo is achieved by means of the Levy flight behaviour equation as illustrated in the following Eqs. 5 and 6 respectively.

$$I_d(\mathrm{t}+1) = \quad (\mathrm{t}) + \alpha \oplus levy(\lambda), \alpha > 0 \tag{5}$$

$$levy(\lambda) = t(-\lambda), 0 to \alpha \tag{6}$$

Table 2 PSNR value at Different Noise Variance levels 0.2, 0.3, 0.5, 0.7, and 0.9 (i) Gaussian Noisy images (ii) Impulse Noisy images

(i)

Noise Variance (σ^2)	PSNR					
	Noise Image (in dB)	Hybrid filter with AGA	Existing DWT	Existing Shrinkage	Existing OGHP	Proposed
0.3	64.44814	63.97303	64.28292	64.24659	64.25562	73.88974
	65.05175	63.58653	63.9498	63.13811	63.11585	73.48641
	64.32195	60.58958	60.67251	59.72662	59.75494	73.87471
	65.04658	62.76044	63.14685	63.28298	63.33635	73.29321
	64.29541	63.44596	63.63928	62.04991	62.07606	74.13385
0.5	60.86993	60.831	60.79807	60.78873	60.83294	71.81826
	61.92622	61.52378	61.41866	61.37984	61.37027	71.47668
	60.52255	58.87675	58.76829	58.50451	58.52071	71.95222
	62.08142	61.75956	61.6475	62.06953	62.14428	71.44236
	61.12374	61.09529	60.91526	60.67069	60.69766	72.00876
0.7	58.89743	58.95162	58.83814	58.85967	58.87758	70.67754
	60.40866	60.3365	60.20035	60.25532	60.25402	70.38115
	58.44113	57.98807	57.90988	57.87773	57.87553	70.66994
	60.75548	60.78647	60.57596	60.78824	60.80872	70.36764
	60.01844	60.0573	59.93259	60.02927	60.04645	69.65676
0.9	58.00647	58.05701	57.99711	58.02289	58.02011	68.92696
	59.8928	59.89313	59.84854	59.87055	59.86568	68.57565
	57.70218	57.68182	57.64957	57.65589	57.65462	68.89613
	60.25383	60.29594	60.2199	60.25509	60.26069	68.54495
	59.80399	59.81801	59.79528	59.82167	59.82368	68.89552

(ii)

Noise Variance (σ2)	PSNR					
	Noise Image (in dB)	Hybrid filter with AGA	Proposed DWT	Existing Shrinkage	Existing OGHP	Proposed
0.2	65.99835	65.13091	65.65767	65.86898	65.7491	85.71914
	66.15485	62.9683	63.44368	62.86547	62.85466	88.58494
	66.00473	62.78244	63.19261	61.88242	61.89405	84.72655
	66.24568	61.23735	61.73409	61.43292	61.46109	82.15146
	66.58026	64.34374	64.9742	63.68144	63.62801	88.94423
0.3	64.24506	63.8368	64.06299	64.0577	64.06115	84.63425
	64.35173	62.32455	62.58441	62.18927	62.25663	86.86455
	64.39767	62.12621	62.41752	61.39817	61.45327	83.45946
	64.3502	60.84574	61.29756	61.06513	61.10014	80.92786
	64.92546	63.49884	63.85056	62.92672	62.9102	87.56129
0.5	62.02659	61.8982	61.93463	61.81374	61.96533	82.78677
	62.16017	61.15657	61.33336	61.13495	61.10833	83.9093
	62.16469	60.94497	61.18714	60.61536	60.62897	81.51007
	62.17552	60.36759	60.58729	60.42468	60.48635	79.66858
	62.71764	62.00984	62.1994	61.74867	61.74881	85.4613
0.7	60.5306	60.51502	60.54263	60.61422	60.47595	81.0639
	60.70011	60.20977	60.30265	60.19948	60.15897	81.9626
	60.65426	60.18311	60.22518	59.96116	59.98384	79.39127
	60.71482	59.8257	59.93303	59.89886	59.88155	78.03081
	61.28069	60.88608	60.9927	60.77734	60.80193	83.26388
0.9	59.46789	59.41279	59.44919	59.49112	59.45517	78.26436
	59.60218	59.47572	59.46829	59.4343	59.45672	77.13468
	59.54694	59.38889	59.41617	59.35702	59.38278	77.24404
	59.64383	59.3837	59.43287	59.41972	59.39804	76.20824
	59.55174	59.35534	59.42325	59.45922	59.46308	75.4575

In the innovative customized cuckoo search technique, arbitrary values are chosen for λ.

Fitness calculation

At the outset, the fitness is evaluated by means of the fitness function with the intention of achieving an optimum solution. Now an arbitrary nest is selected, which is termed as j.

$$fitness = \max(PSNR)$$

Subsequently, the fitness of the cuckoo egg (new solution) is appraised and contrasted with those of the host eggs (solutions) existing in the nest. If the value of the fitness function of the cuckoo egg falls within or is equivalent to that of the arbitrarily selected nest, then the arbitrarily selected nest (j) is substituted by the new solution.

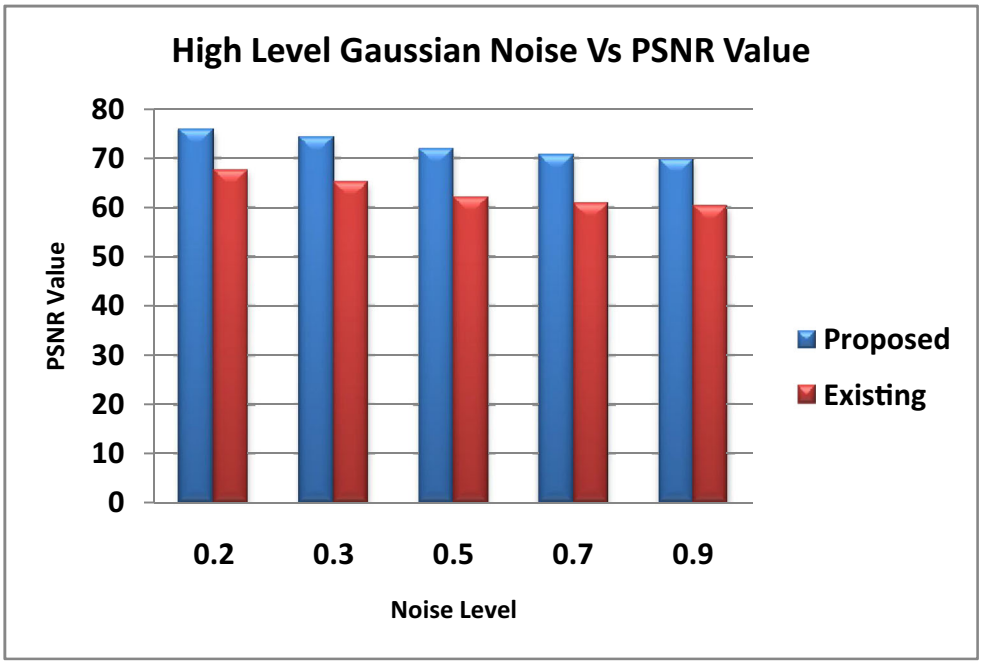

(i)

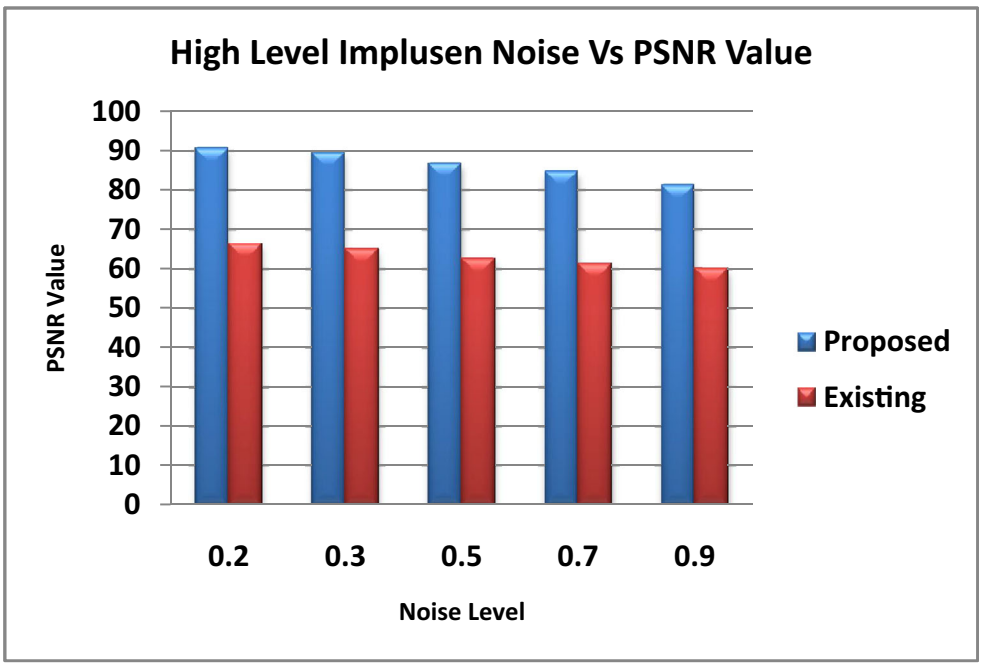

(ii)

Fig. 8 Comparison of proposed and existing methods in terms of PSNR value by varying noise levels (i) Gaussian Noise (ii) Impulse Noise

Termination If the algorithm is terminated subsequent to attainment of the maximum number of generations, it is possible that a suitable solution is achieved or not.

Combining image using DWT

The optimized Gradient Histogram Preservation (OGHP) and shrinkage are fused by the discrete wavelet transform.

Table 3 SSIM value of our proposed method and the different existing methods results for different noise level (i) Gaussian noise denoised image (ii) Impulse noise denoised image

(i)

Noise Variance (σ^2)	SSIM					
	Noise Image (in dB)	Hybrid filter with AGA	Proposed DWT	Existing Shrinkage	Existing OGHP	Proposed
0.2	0.995176	0.995093	0.995001	0.994859	0.994974	0.999209
	0.995153	0.987396	0.987168	0.986763	0.98648	0.999162
	0.994145	0.972479	0.972176	0.971916	0.971819	0.999248
	0.995167	0.993453	0.993817	0.99281	0.992739	0.999177
	0.994257	0.98702	0.986907	0.98684	0.986851	0.999265
0.3	0.990482	0.990246	0.989862	0.990053	0.990093	0.998925
	0.99037	0.98265	0.982435	0.984579	0.984642	0.99883
	0.987365	0.962761	0.962289	0.964627	0.964996	0.99894
	0.990251	0.990603	0.990268	0.992121	0.992262	0.99887
	0.987832	0.981128	0.980311	0.98101	0.981316	0.998973
0.5	0.980798	0.98089	0.979892	0.980004	0.980039	0.998305
	0.979098	0.973326	0.972266	0.979074	0.978948	0.99822
	0.968054	0.949121	0.947395	0.952824	0.952455	0.998429
	0.979531	0.981738	0.979774	0.985277	0.985448	0.998303
	0.973782	0.970906	0.969606	0.970816	0.971175	0.998233
0.9	0.973857	0.973852	0.973748	0.973793	0.973807	0.996977
	0.967543	0.967222	0.967165	0.967809	0.967764	0.996885
	0.942723	0.942221	0.942147	0.942399	0.942373	0.997026
	0.972453	0.972627	0.972373	0.972756	0.972674	0.996864
	0.965697	0.965659	0.96563	0.965645	0.965656	0.996903

(ii)

Noise Variance (σ^2)	SSIM					
	Noise Image (in dB)	Hybrid filter with AGA	Existing DWT	Existing Shrinkage	Existing OGHP	Proposed
0.2	0.998495	0.998369	0.998389	0.998421	0.998667	0.999956
	0.998637	0.990474	0.991055	0.987943	0.987577	0.999983
	0.998578	0.989083	0.989379	0.986494	0.98668	0.999944
	0.998711	0.992539	0.993618	0.987283	0.98722	0.99991
	0.998798	0.995413	0.995723	0.994163	0.993947	0.999984
0.3	0.997449	0.997662	0.997772	0.997554	0.99788	0.999942
	0.997539	0.990606	0.990661	0.988131	0.988328	0.999971
	0.997768	0.988946	0.989467	0.987306	0.987227	0.999918
	0.99793	0.992308	0.992489	0.988655	0.988213	0.999878
	0.998125	0.995146	0.995291	0.994777	0.994772	0.999976
0.5	0.995373	0.996147	0.995848	0.995552	0.996396	0.999902
	0.995913	0.9902	0.990547	0.98924	0.98896	0.99993
	0.99593	0.988654	0.989366	0.988615	0.987903	0.999865
	0.996293	0.992446	0.992481	0.989238	0.989335	0.999818
0.9	0.991389	0.990761	0.988418	0.98867	0.987883	0.999653
	0.990181	0.988821	0.989019	0.989329	0.989708	0.99957
	0.990845	0.989369	0.990849	0.990527	0.990057	0.999638
	0.992028	0.991218	0.9936	0.993914	0.993119	0.999505
	0.994078	0.994203	0.990484	0.990651	0.991256	0.999789

The denoised images are represented as I_1andI_2.The discrete wavelet transform (DWT) represents a linear transformation which functions on a data vector whose length constitutes an integer power of two, converting it

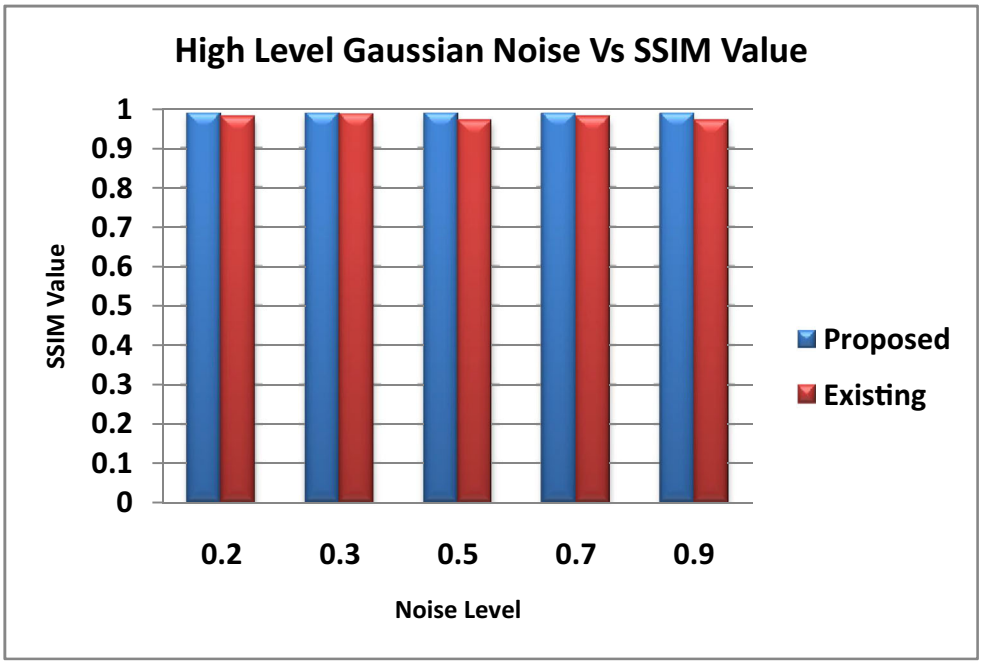

(i)

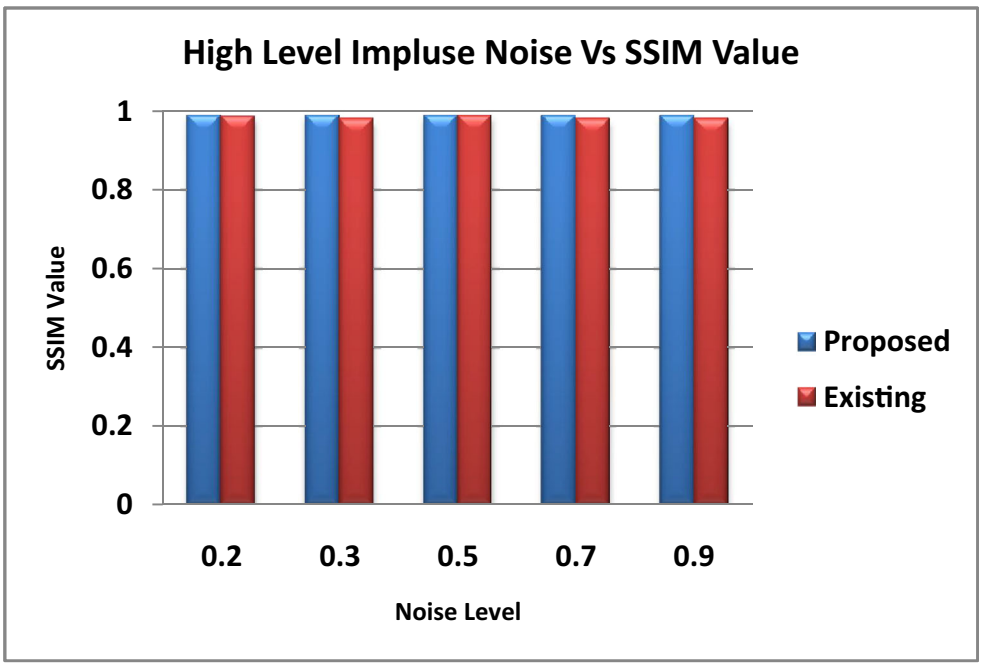

(ii)

Fig. 9 Comparison of SSIM value of the proposed technique with that of the existing techniques by varying the high level noise range (i) Gaussian noise denoised image (ii) Impulse noise denoised image

into a numerically different vector of the identical length. It represents a device that divides the data into various frequency segments, and thereafter investigates each component with resolution harmonized to its scale. The DWT [3] is evaluated with a cascade of filtering accompanied by a factor 2 sub sampling.

In wavelet image fusing technique, the source images $I_1(x, y)$ and $I_2(x, y)$, are decayed into the approximation and

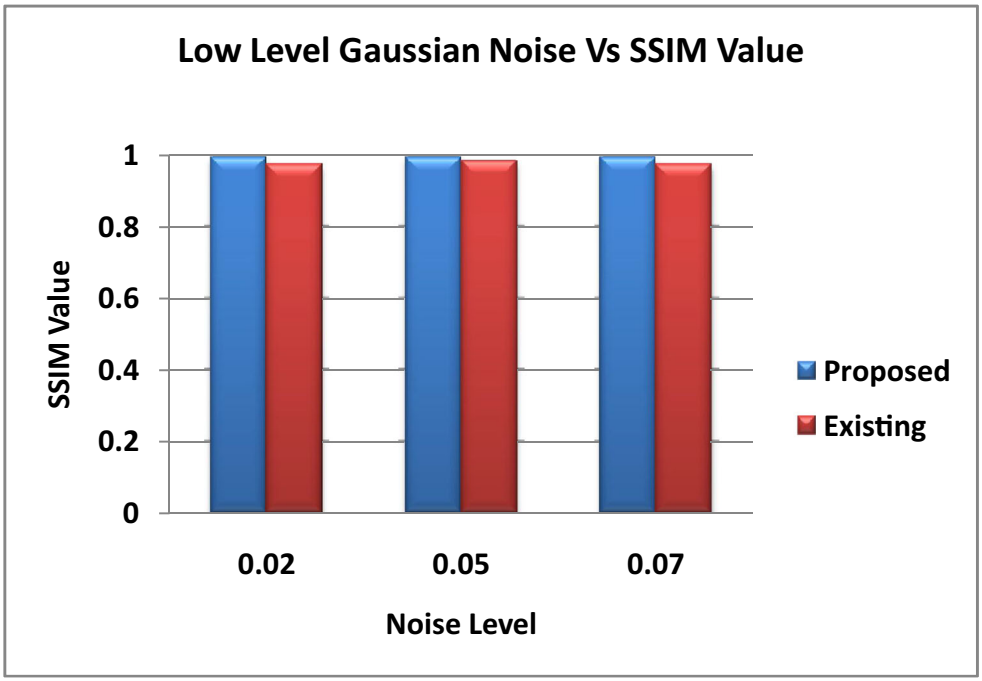

(i)

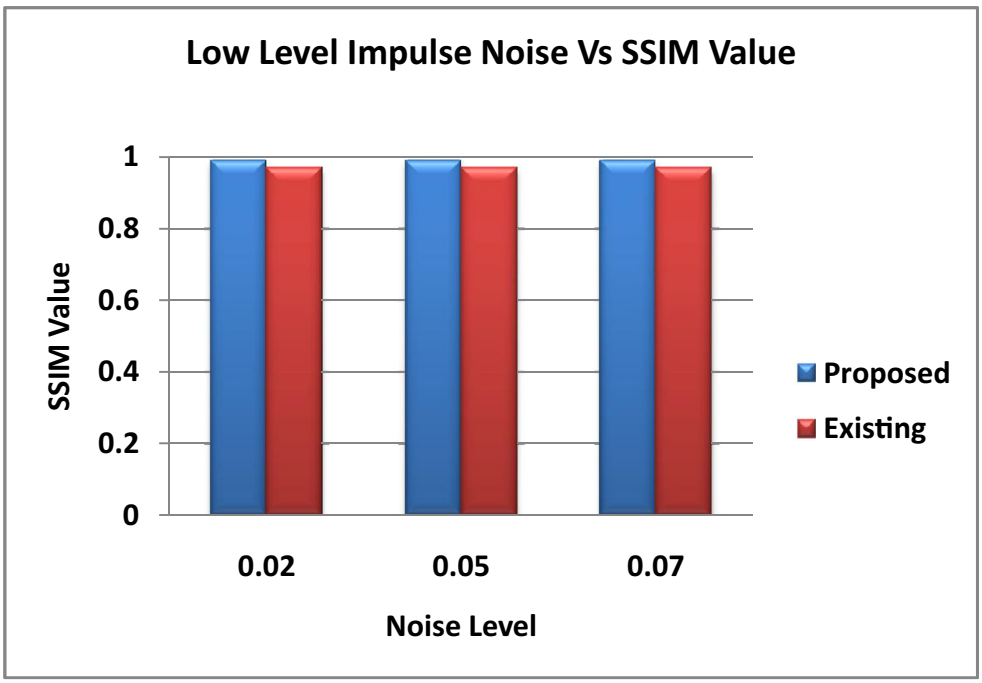

(ii)

Fig. 10 Comparison of SSIM value of the proposed technique with that of the existing techniques by varying the low level noise range (i) Gaussian noise denoised image (ii) Impulse noise denoised image

comprehensive coefficients at the preferred level with the help of the DWT.The integrated image $I_f(x, y)$ is attained by taking the inverse discrete wavelet transform (IDWT). The current and the upcoming sections are also detailed in the previous paper.

Table 4 Proposed and different filtering methods SSIM value of three Different Noise Variance levels 0.02, 0.05 and 0.07 (i) Gaussian Noisy images (ii) Impulse Noisy images

Noise Variance (σ^2)	SSIM					
	Noise Image (in dB)	Hybrid filter with AGA	Proposed DWT	Existing Shrinkage	Existing OGHP	Proposed
(i)						
0.02	0.994859	0.995176	0.995001	0.994974	0.995093	0.999893
	0.986763	0.995153	0.987168	0.98648	0.987396	0.999894
	0.971916	0.994145	0.972176	0.971819	0.972479	0.99989
	0.99281	0.995167	0.993817	0.992739	0.993453	0.999879
	0.98684	0.994257	0.986907	0.986851	0.98702	0.9999
0.05	0.990053	0.990482	0.989862	0.990093	0.990246	0.999766
	0.984579	0.99037	0.982435	0.984642	0.98265	0.999769
	0.964627	0.987365	0.962289	0.964996	0.962761	0.999774
	0.992121	0.990251	0.990268	0.992262	0.990603	0.999757
	0.98101	0.987832	0.980311	0.981316	0.981128	0.99978
0.07	0.980004	0.980798	0.979892	0.980039	0.98089	0.999682
	0.979074	0.979098	0.972266	0.978948	0.973326	0.999684
	0.952824	0.968054	0.947395	0.952455	0.949121	0.999702
	0.985277	0.979531	0.979774	0.985448	0.981738	0.999679
(ii)						
0.02	0.992739	0.995176	0.995001	0.994974	0.995093	0.999984
	0.986851	0.995153	0.987168	0.98648	0.987396	0.999992
	0.986097	0.994145	0.972176	0.971819	0.971916	0.999974
	0.980597	0.995167	0.993817	0.992739	0.99281	0.999951
	0.993858	0.994257	0.986907	0.986851	0.98684	0.999994
0.05	0.992262	0.990482	0.989862	0.990093	0.990053	0.999982
	0.981316	0.99037	0.982435	0.984642	0.984579	0.999991
	0.978988	0.987365	0.962289	0.964996	0.964627	0.999975
	0.973041	0.990251	0.990268	0.992262	0.992121	0.999943
	0.991565	0.987832	0.980311	0.981316	0.98101	0.999992
0.07	0.985448	0.980798	0.979892	0.980039	0.98089	0.99998
	0.971175	0.979098	0.972266	0.978948	0.973326	0.99999
	0.964656	0.968054	0.947395	0.952455	0.949121	0.999971
	0.955167	0.979531	0.979774	0.985448	0.981738	0.999938
	0.975361	0.978121	0.967407	0.974973	0.968136	0.999985

Image restoration using AGA

The noiseless image $I_f^{'}$ attained from the hybrid filter appears to be distorted, hence it is highly essential to fine-tune the quality of the image. With an eye on boosting the noiseless image quality, we have resorted to the deployment of AGA method along with Richardson-Lucy (R-L) algorithm. In the image restitution procedure, the all-powerful Point Spread Function (PSF) is entrusted with the task of carrying out successful restitution. The optimized PSF by means of our new-fangled AGA is advantageous to the RL algorithm for restoring the distorted image. The modus operandi of AGA regarding PSF calculation is detailed as follows:

Initialization At the outset, a chromosome h_i; $0 \le i \le n_c$ is engendered, where n_c represents the total number of produced chromosomes. The chromosomes gene values arbitrarily are created in the range of [0, 1]. In this case, 10 matrices are randomly generated to give shape to the preliminary population. The engendered chromosomes are assessed in accordance with their fitness function. The estimations of fitness function for the engendered chromosomes are carried out as follows:

Table 5 PSNR, SSDM, SSIM value of proposed and existing techniques with noise variance 0.02 and 0.2(i) Gaussian Noisy images (ii) Impulse Noisy images

Noise Variance (σ^2)	Image	PSNR			SDME			SSIM		
		Proposed	CSA	GA	Proposed	CSA	GA	Proposed	CSA	GA
(i)										
0.02	1	82.87	81.97	80.52	80.59	72.57	76.43	0.9998930	0.9998	0.99984
	2	82.58	81.33	80.44	93.56	81.42	81.35	0.9998943	0.9987	0.99985
	3	82.37	81.57	80.52	77.5	80.57	74.01	0.99989	0.9998	0.99985
	4	81.37	80.90	79.74	79.32	81.73	85.34	0.9998792	0.9998	0.99983
	5	83.13	81.9	80.71	96.68	82.19	87.39	0.9999001	0.9998	0.99985
	6	83.00	81.54	80.66	84.14	91.71	80.22	0.9998978	0.9998	0.99985
	7	82.28	81.60	80.36	80.43	82.16	85.33	0.9998879	0.9998	0.99984
	8	84.80	82.68	81.09	78.35	90.67	80.66	0.9999263	0.9998	0.99986
	9	83.83	82.23	80.81	91.04	86.46	83.40	0.9999157	0.9998	0.99986
	10	82.51	81.50	80.29	98.16	92.66	82.54	0.9998926	0.9998	0.99984
	Avg.	82.883	81.72	80.52	85.98	84.21	77.13	0.9998977	0.9998	0.99985
0.2	1	75.21	72.89	72.31	75.91	68.44	76.43	0.9998930	0.9998	0.99984
	2	74.80	72.92	72.23	77.70	74.42	81.35	0.9998943	0.9987	0.99985
	3	75.17	72.92	72.34	70.65	70	74.01	0.99989	0.9998	0.99985
	4	74.56	72.53	72.09	73.05	73.87	85.34	0.9998792	0.9998	0.99983
	5	75.61	72.79	72.17	79.38	73.24	87.39	0.9999001	0.9998	0.99985
	6	75.46	73.05	72.31	67.76	73.20	80.22	0.9998978	0.9998	0.99985
	7	74.94	73.02	72.42	72.45	71.82	85.33	0.9998879	0.9998	0.99984
	8	75.81	72.16	72.53	79.43	70.99	80.66	0.9999263	0.9998	0.99986
	9	75.65	72.76	72.31	78.21	72.58	83.40	0.9999157	0.9998	0.99986
	10	74.93	72.93	72.25	75.88	73.39	82.54	0.9998926	0.9998	0.99984
	Avge.	75.2189	72.85	72.30	75.04	69.19	77.13	0.9998977	0.9998	0.99985
(ii)										
0.02	1	89.08	88.54	80.52	80.59	88.29	76.43	0.99989306	0.99998	0.99984
	2	91.14	90.11	80.44	93.56	99.81	81.35	0.9998943	0.99999	0.99985
	3	87.51	87.0	80.52	77.52	76.60	74.01	0.99989	0.99997	0.99985
	4	84.21	83.75	79.74	79.32	92.06	85.34	0.99987924	0.99994	0.99983
	5	91.85	91.40	80.71	96.68	88.61	87.39	0.99990011	0.99993	0.99985
	6	92.85	92.09	80.66	84.145	92.68	80.22	0.99989781	0.99999	0.99985
	7	86.69	86.17	80.36	80.43	78.04	85.33	0.99988794	0.99999	0.99984
	8	92.52	91.94	81.09	78.35	76.66	80.66	0.99992636	0.99999	0.99986
	9	90.47	89.95	80.81	91.04	91.09	83.40	0.99991574	0.99996	0.99986
	10	86.59	86.53	80.29	98.16	93.00	82.54	0.9998926	0.99972	0.99984
	Avge.	89.29	88.75	80.52	85.98440	87.68	77.13	0.99989772	0.99997	0.99985
0.2	1	85.71	85.94	84.71	94.09	90.09	81.88	0.999956	0.99996	0.99994
	2	88.58	87.91	85.34	90.41	92.41	92.58	0.999983	0.99997	0.99995
	3	84.72	84.48	84.57	80.68	80.08	73.16	0.999944	0.99993	0.99995
	4	82.15	81.68	82.27	96.26	88.26	90.32	0.999912	0.99990	0.99992
	5	88.94	85.84	85.79	87.88	84.88	89.61	0.999984	0.99997	0.99996
	6	88.21	88.28	85.17	79.22	74.22	82.60	0.999977	0.99992	0.99996
	7	83.76	83.96	83.04	81.92	81.92	80.01	0.999926	0.99998	0.99993
	8	90.73	90.26	86.72	83.817	82.81	86.32	0.999988	0.99998	0.99997
	9	87.62	87.34	85.39	92.07	90.07	84.59	0.999974	0.99997	0.99996
	10	83.93	82.93	85.03	77.67	90.67	80.22	0.999923	0.99992	0.99996
	Avge.	86.43975	85.94	84.80	87.4054	85.40	84.13	0.999957	0.99995	0.99995

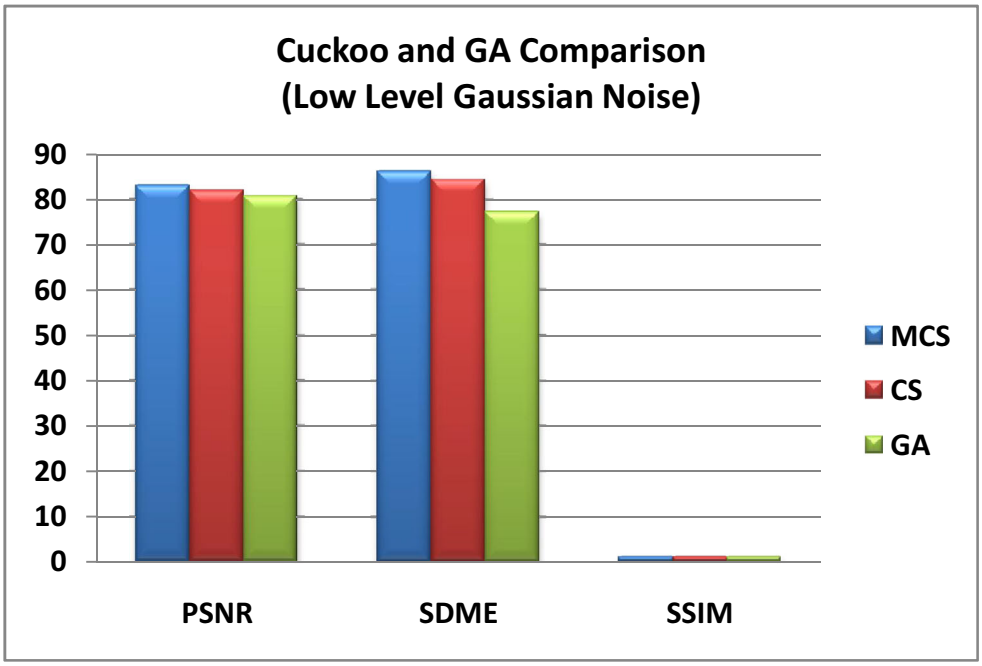

(i)

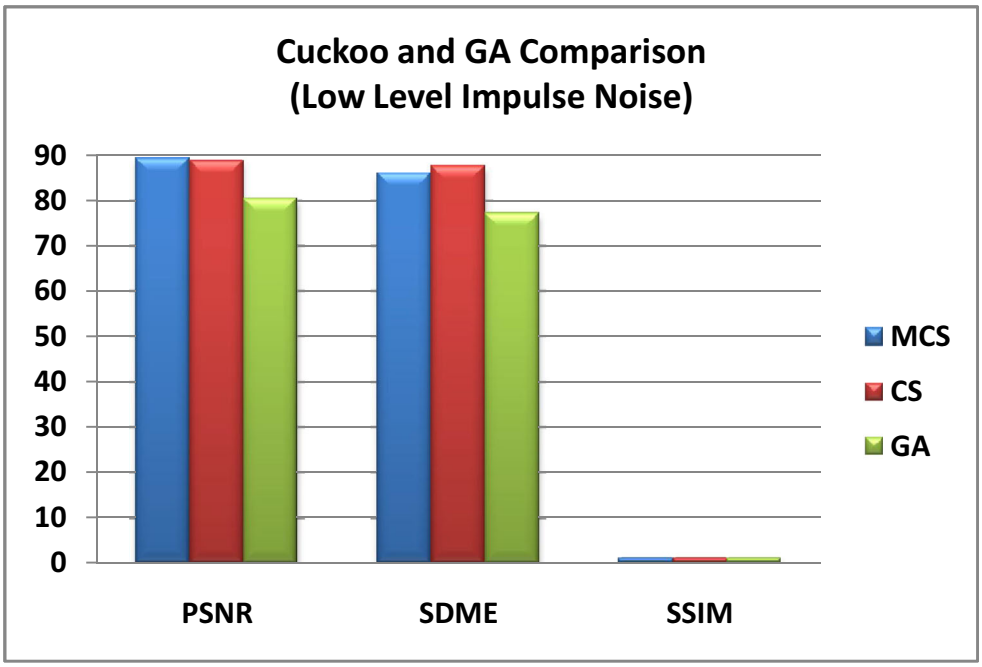

(ii)

Fig. 11 Comparison of image restoration performance of the proposed and the existing techniques at noise level 0.02 (i) Impulse noise added image (ii) Gaussian noise added image

Fitness function The chromosomes fitness function is evaluated by means of the following Relation:

$$SDME = -\frac{1}{b_1.b_2}\sum_{i=1}^{b_1}\sum_{j=1}^{b_2} 20\ln\left|\frac{p_{\max,j,i}-2p_{cen,j,i}+p_{\min,j,i}}{p_{\max,j,i}+2p_{cen,j,i}+p_{\min,j,i}}\right|$$

It represents an enhancement measure integrating the theory of the second-derivative. Let us presume that the image $I_f^{'}$ is divided into $b_1 \times b_2$ blocks, and $p_{\max,\ j,\ i}$, $p_{\min,\ j,\ i}$ represent the maximum and minimum values of

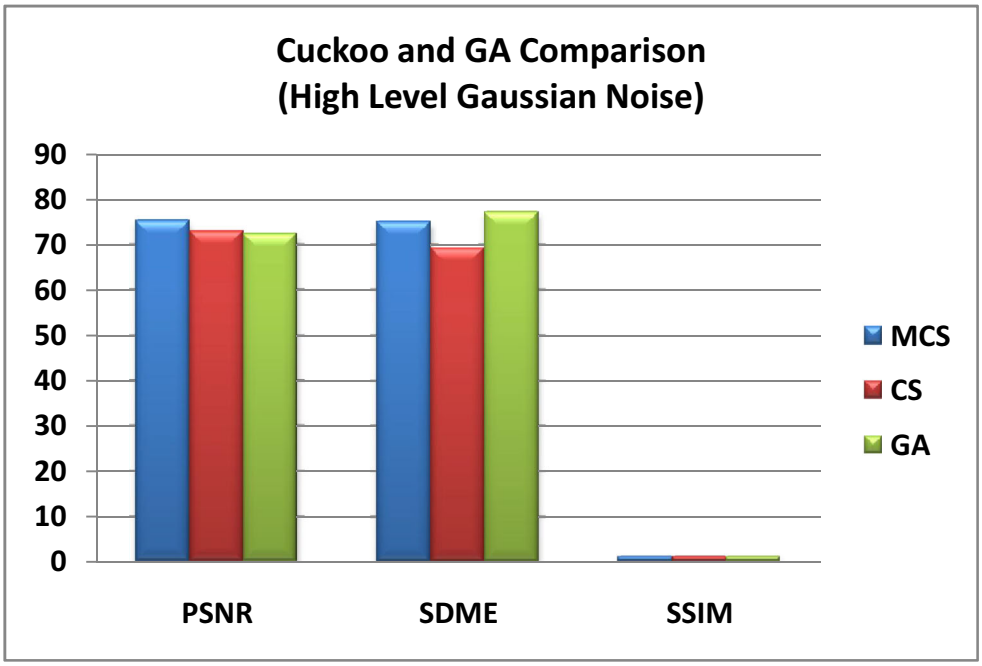

(i)

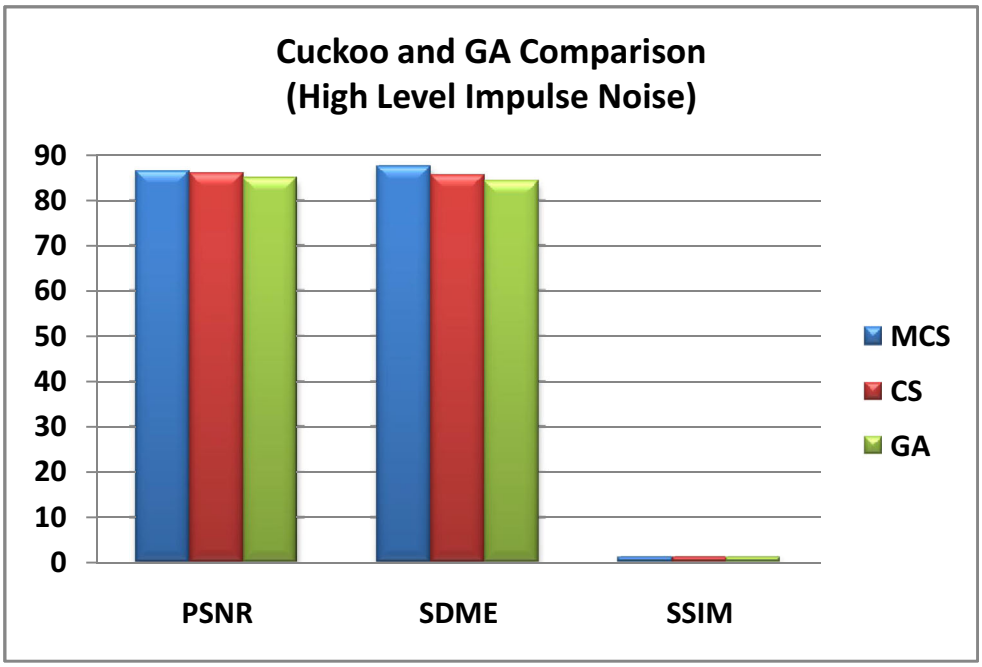

(ii)

Fig. 12 Comparison of PSNR, SSDM, SSIM values of the proposed and conventional algorithms CS and GA at noise level 0.2 (i) Gaussian Noisy images (ii) Impulse Noisy images

the pixels in each block independently, and $p_{cen,\ j,\ i}$ represents the intensity of the center pixel in each block.

Probability of crossover and mutation When the fitness function evaluation is completed, the chromosomes are crossed and mutated in accordance with their crossover and mutation rates.

In the novel AGA, both these rates are evaluated by employing their fitness values from the population. The newly created probability based crossover and mutation rates are effectively utilized in the crossover and mutation rates evaluation process.

Termination If the technique is terminated after attainment of the maximum number of generations, it is possible that a fitting solution is achieved or not. As a result, the optimized PSF from the AGA is effectively deployed in the RL technique for regaining the tainted image further proficiently.

Richardson-Lucy algorithm

The Richardson-Lucy (R-L) technique effectively utilizes an innovative probabilistic technique for regaining the tainted image. At this juncture, the contaminated image $d_f^{'}$ is fed as input, and an image k which maximizes the chances of supervising the image $d_f^{'}$ is found out. Considering the image as an analysis of a Poisson process, the probability function is defined as:

From the above equation, a functional to be deducted, $L(\hat{k}) = -\log p(I^{'}|k)$ is obtained, representing the maximum probability estimate as:

An iterative technique is expected to be achieved from the above functional. It is known as the Richardson-Lucy technique and is expressed by:

The relative technique comes to an end after a preset number of iterations. When the de-convolution is ill-posed, which habitually occurs in the genuine applications, the signal-to-noise ratio exhibits a tendency to emerge as extremely inferior to the number of iterations $n \rightarrow \infty$. In RL technique, a set of functions is carried out for a fixed number of iterations and at last, we come face to face with the anticipated, enhanced and reclaimed image $d_f^{'}$.

Experimental results and discussion

The novel heuristic method is performed in the working platform of the MATLAB version 7.14 together with the classification GUI (Graphical User Interface) which is furnished for both the Gaussian and salt and pepper noise categories. The input image is denoised with the help of the innovative hybrid Adaptive median filter and the adaptive fuzzy switching with the AGA technique. Further, the denoised image is regained by the AGA (Richard-Lucy technique). The sample input images employed in the new-fangled approach are effectively exhibited in Fig. 2.

Well-before the start of the noise elimination procedure, the impulse noise and Gaussian noises are included in the image. The figure appearing below illustrates the samples of noise-added images.

Figures 3 and 4 Noise Added Images (3) Image with Gaussian Noise (4) Image with impulse noise. These noise affected images are de-noised using optimized texture and Shrinkage. Thus the noise removed images are shown in Fig. 5.

Now the noise-free images are furnished to the DWT for merging and later on subjected to the AGA image restoration procedure. The image obtained from the AGA restoration procedure is effectively exhibited in Fig. 6.

Performance analysis

The functioning of the novel method is effectively appraised with the help of two efficiency metrics such as PSNR, and SSIM by duly modulating the Gaussian and impulse noises as 0.02, 0.05 and 0.07. In addition, the feat of the novel method is assessed and contrasted with those of the modern filter and optimization approaches. In this connection, the noise elimination feat of the novel technique together with those of the modern filter based approaches with respect to their PSNR values are effectively furnished in Table 1.

The average PSNR value computed from the above tables are represented as graphs in Fig. 7.

Figure 7 illustrates the performance of the noise removal process of both the existing and the proposed technique at the regular intervals of noise levels 0.02, 0.05and 0.07. While looking the Fig. 7(i), the PSNR value of the proposed and that of the existing technique looks like similar. But the PSNR value of the proposed technique is slightly higher than the existing technique except noise level at 0.07. Figure 7(ii) shows the PSNR value obtained while varying the impulse noise levels. Here the PSNR value of the proposed technique beats the existing technique's PSNR value. The PSNR value of the proposed technique is nearer to 90 which is greater than the existing technique.

The noise removal performance of both the proposed method and the existing methods by varying the noise levels at noise removal stage, merging stage and restoration stage in terms of their PSNR value is given in Table 2.

In Fig. 8(i) and (ii), shows the comparison graph of proposed method, and the existing methods in the Gaussian and impulse noise removal process. The graphs are drawn by taking the average values of the PSNR values mentioned in Table 2. From the Fig. 8, we can see that the PSNR average PSNR value of the proposed technique is higher than that of the existing technique. Even though the PSNR value decreases as the noise level increases, proposed technique's PSNR value is still higher. Thus we proved that the proposed technique performance is better than the existing technique in the noise removal process.

After that, the image restoration performance is evaluated by computing SSIM measure on the restored images. The restored images results obtained from the different noise variance levels are given in Table 3.

Figure 9 illustrates the performance of image restoration by taking the average of SSIM given in Table 3 for the existing and the proposed technique at the regular intervals of high

level noise 0.2, 0.3, 0.5, 0.7 and 0.09. On looking at the graph, we can say that the SSIM value of the proposed technique is higher than that of the existing technique.

The average PSNR value of our proposed method and those of the different existing methods for the different noise variance level comparison graph are illustrated in Fig. 10.

In Fig. 10(i) and (ii), shows the comparison graph of proposed method, and the existing methods in the image restoration process. The graphs are drawn by taking the average values of the SSIM values mentioned in Table 4. From the Fig. 10, eventhough the SSIM values of both the existing and the proposed technique look similar, there is a slight variation between them.

Table 5 shows the proposed technique performance in terms of PSNR, SDME and SSIM. Moreover, our proposed technique performance is compared with the Existing GA and optimization methods (Cuckoo search Algorithm).

Figure 11 shows the comparison of image restoration performance of our proposed modified cuckoo search algorithm and other optimization methods GA and Cuckoo search Algorithm. The picture is depicted by taking the average values taken from Table 5. When compared to the conventional CS and GA algorithms, our proposed modified CS algorithm attained higher value in all the measures such as PSNR, SSIM and SDME. Higher value indicates higher performance. Thus high value of PSNR, SSIM SDME shows the better image restoration performance.

Figure 12 shows the image restoration performance of our proposed AGA and other optimization methods GA and Cuckoo search Algorithm. The high value of PSNR SSIM SDME shows the better image restoration performance. With our proposed denoising technique with AGA, and Cuckoo search Algorithm method has given high image restoration performance than the other filtering methods. In our proposed restoration technique, AGA has given high PSNR SSIM SDME value than the other existing techniques.

Conclusion

In the proposed image restoration technique, initially the preprocessing is carried out by two filters adaptive median filter, adaptive fuzzy switching, and that preprocessed image is given to next step of noise removal process such as (OGHP) and SURE shrinkage. During OGHP noise removal process, GHP parameters are optimized by using modified Cuckoo Search Algorithm. All this process has improved the performance of the noise removal and restoration techniques. The results have shown that the proposed technique has achieved higher PSNR values than the existing and optimization methods. Thus, the proposed techniques has offered better performance in de-noising all type of noisy images with higher de-noising PSNR ratio and restore all images with high quality.

References

1. Sarker, S., Chowdhury, S., Laha, S., and Dey, D., Use Of Non-Local Means Filter To Denoise Image Corrupted By Salt And Pepper Noise. Signal & Image Processing: An International Journal 3(2):223–235, 2012.
2. Cho, T. S., Zitnick, L., Joshi, N., Kang, S. B., Szeliski, R., and Freeman, W., Image Restoration by Matching Gradient Distributions. IEEE Trans. Pattern Anal. Mach. Intell. 34(4):683–694, 2012.
3. Kaur, M., and Sharm, R., Restoration Of Medical Images Using Denoising. International Journal For Science And Emerging Technologies With Latest Trends 5(1):35–38, 2013.
4. George, A., Rajakumar, B. R., and Suresh, B., Markov Random Field based Image Restoration with aid of Local and Global Features. Int. J. Comput. Appl. 48(8):0975–0888, 2012.
5. Lefkimmiatis, S., Bourquard, A., and Unser, M., Hessian-Based Norm Regularization For Image restoration With Biomedical Applications. IEEE Trans. Image Process. 21(3):983–995, 2012.
6. Zheng, S., Pan, Z., Zhao, X., and Wang, G., A General Adaptive Variational Model For Image Restoration Based On First And Second Order Derivatives. Journal Of Computational Information Systems 8(24):10169–10175, 2012.
7. Sakthidasan @ Sankaran, K., Prabha S., and Rubesh Anand, P. M., Optimized gradient histogram preservation with block wise SURE shrinkage for noise free image restoration. *Springer -Cluster Computing- The Journal of Networks, Software Tools and Applications*, 1-22 , ISSN 1573-7543, 2018
8. Zhang, H., Yang, J., Zhang, Y., and Huang, T., Image and Video Restoration via Non-Local Kernel regression. IEEE Transactions on Systems, Man, and Cybernetics–Part B: Cybernetics 42(6):1–12, 2012.
9. Lopez-Rubio, E., Restoration of images corrupted by Gaussian and uniform impulsive noise. Pattern Recogn. 43(5):1835–1846, 2010.
10. Yang, L., Parton, R., Ball, G., Qiu, Z., Greenaway, A., Davis, I., and Lu, W., An adaptive non-local means filter for denoising live-cell images and improving particle detection. J. Struct. Biol. 172(3):233–243, 2010.
11. Lin, T.-C., Decision-based fuzzy image restoration for noise reduction based on evidence theory. Expert Syst. Appl. 38(7):8303–8310, 2011.
12. Lee, C., Lee, C., and Kim, C.-S., An MMSE approach to nonlocal image denoising: Theory and practical implementation. J. Vis. Commun. Image Represent. 23(3):476–490, 2012.
13. Zhang, H., Yang, J., Zhang, Y., and Huang, T. S., Image and Video Restorations via Nonlocal Kernel Regression. IEEE Transactions on Cybernetics 43(3):1035–1046, 2013.
14. Wang, S., Xia, Y., and QiegenLiu, P. D., David Dagan Feng, and Jianhua Luo, Fenchel Duality Based Dictionary Learning for Restoration of Noisy Images. IEEE Trans. Image Process. 22(12):5214–5225, 2013.
15. Dong, W., Zhang, L., Shi, G., and Li, X., Nonlocally Centralized Sparse Representation for Image Restoration. IEEE Trans. Image Process. 22(4):1620–1630, 2013.
16. Rasti, B., Sveinsson, J. R., and Ulfarsson, M. O., Wavelet-Based Sparse Reduced-Rank Regression for Hyperspectral Image Restoration. IEEE Trans. Geosci. Remote Sens. 52(10):6688–6698, 2014.